inorganics

MDPI

Article

Mono- and Hexanuclear Zinc Halide Complexes with Soft Thiopyridazine Based Scorpionate Ligands

Michael Tüchler [1], Melanie Ramböck [1], Simon Glanzer [2], Klaus Zangger [2], Ferdinand Belaj [1] and Nadia C. Mösch-Zanetti [1,*]

1 Institute of Chemistry, Inorganic Chemistry, University of Graz, Schubertstrasse 1, 8010 Graz, Austria; michael.tuechler@uni-graz.at (M.T.); melanie.ramboeck@edu.uni-graz.at (M.R.); ferdinand.belaj@uni-graz.at (F.B.)

2 Institute of Chemistry, Organic and Bioorganic Chemistry, University of Graz, Heinrichstrasse 28, 8010 Graz, Austria; simon.glanzer@uni-graz.at (S.G.); klaus.zangger@uni-graz.at (K.Z.)

* Correspondence: nadia.moesch@uni-graz.at

Received: 20 December 2018; Accepted: 5 February 2019; Published: 19 February 2019

Abstract: Scorpionate ligands with three soft sulfur donor sites have become very important in coordination chemistry. Despite its ability to form highly electrophilic species, electron-deficient thiopyridazines have rarely been used, whereas the chemistry of electron-rich thioheterocycles has been explored rather intensively. Here, the unusual chemical behavior of a thiopyridazine (6-*tert*-butylpyridazine-3-thione, H$^{t\mathrm{Bu}}$Pn) based scorpionate ligand towards zinc is reported. Thus, the reaction of zinc halides with tris(6-*tert*-butyl-3-thiopyridazinyl)borate Na[Tn$^{t\mathrm{Bu}}$] leads to the formation of discrete torus-shaped hexameric zinc complexes [Tn$^{t\mathrm{Bu}}$ZnX]$_6$ (X = Br, I) with uncommonly long zinc halide bonds. In contrast, reaction of the sterically more demanding ligand K[Tn$^{\mathrm{Me},t\mathrm{Bu}}$] leads to decomposition, forming Zn(HPn$^{\mathrm{Me},t\mathrm{Bu}}$)$_2X_2$ (X = Br, I). The latter can be prepared independently by reaction of the respective zinc halides and two equiv of HPn$^{\mathrm{Me},t\mathrm{Bu}}$. The bromide compound was used as precursor which further reacts with K[Tn$^{\mathrm{Me},t\mathrm{Bu}}$] forming the mononuclear complex [Tn$^{\mathrm{Me},t\mathrm{Bu}}$]ZnBr(HPn$^{\mathrm{Me},t\mathrm{Bu}}$). The molecular structures of all compounds were elucidated by single-crystal X-ray diffraction analysis. Characterization in solution was performed by means of ^{1}H, ^{13}C and DOSY NMR spectroscopy which revealed the hexameric constitution of [Tn$^{t\mathrm{Bu}}$ZnBr]$_6$ to be predominant. In contrast, [Tn$^{\mathrm{Me},t\mathrm{Bu}}$]ZnBr(HPn$^{\mathrm{Me},t\mathrm{Bu}}$) was found to be dynamic in solution.

Keywords: soft scorpionate; zinc; hexanuclear compounds

1. Introduction

The use of borate-based ligands in coordination chemistry has gained significant attention over the last 50 years, when Trofimenko introduced the ligand class of scorpionates [1–3]. In particular, substituted polypyrazolyl borates have been widely used for the biomimetic modelling of nitrogen-rich active sites, as they enforce a facial coordination and thus allow mimicking of a tetrahedral geometry [1,4,5]. In addition, sulfur donating scorpionates, in which the pyrazolyl moiety is replaced by a thioheterocycle such as methimidazole [6], thiopyridine [7] or thiopyridazine [8], were developed. Such ligands, first introduced by Reglinski and coworkers [9], exhibit soft coordination properties, thereby significantly enlarging the scope of this chemistry.

Recently, we introduced a new electron-deficient thiopyridazine based soft scorpionate ligand and investigated its coordination behavior towards cobalt, nickel [8] and copper [10,11]. We found that the electron deficiency of this ligand class leads to new reactivity compared to more electron-rich analogues. This is demonstrated by the high tendency to form boratrane compounds with a direct metal boron interaction [8,10,11]. Furthermore, the pyridazine based scorpionate ligands exhibit photochemical

reactivity, as observed with potassium hydrotris(6-*tert*-butyl-3-thiopyridazinyl)borate K[Tn$^{t\mathrm{Bu}}$] which is, upon exposure to light, transformed into 2 equiv of 6-*tert*-butylpyridazine-3-thione and 1 equiv of 4,5-dihydro-6-*tert*-butylpyridazine-3-thione [12]. The parent 6-*tert*-butylpyridazine-3-thione is redox-active in presence of iron(II) under formation of di-organotrisulfide based iron complexes and concomitant C–N-coupled, desulfurized pyridazinyl-thiopyridazines [13]. The iron compounds exhibit unusually high redox potentials due to the electron-deficiency of the pyridazine heterocycle.

Inspired by the tris-histidine site of the active site of Carbonic Anhydrase, much effort has been placed into the synthesis and structural characterization of zinc complexes that contain trispyrazolyl borate ligands [4,14–17]. Since in several other zinc enzymes, the metal is—beside histidine—coordinated by cysteine, a number of sulfur-based scorpionate zinc complexes have also been reported [9,18–20]. The electron-deficient pyridazine heterocycle is expected to enhance the Lewis acidity of the zinc center promoting interesting reactivity which prompted us to investigate the coordination chemistry of thiopyridazine based scorpionate ligands towards zinc. With zinc, a boratrane complex is not feasible, as boratrane complexes may be formed by reaction of a borate ligand and a metal salt under reduction of the metal which is not an option with zinc. On the other hand, tris(thiopyridazinyl) scorpionate ligands, in which the borate backbone is replaced by carbon, allow the preparation of various mononuclear zinc complexes with a direct zinc carbon bond [21,22]. Furthermore, we previously have observed that the hybrid thiopyridazine-methimazole scorpionate ligand forms a bridging, dinuclear species [23]. For these reasons, we were interested in whether the borate scorpionate ligands Na[Tn$^{t\mathrm{Bu}}$] or Na[Tn$^{\mathrm{Me},t\mathrm{Bu}}$] can coordinate to zinc in order to form mononuclear complexes.

Here, the reactivity of electron-deficient hydrotris-(6-*tert*-butyl-3-thiopyridazinyl) borate (Tn$^{t\mathrm{Bu}}$) and hydrotris-(6-*tert*-butyl-4-methyl-3-thiopyridazinyl) borate (Tn$^{\mathrm{Me},t\mathrm{Bu}}$) scorpionate ligands towards zinc halides is reported with the former ligand forming a novel, neutral, three-dimensional hexameric cage structure.

2. Results and Discussion

2.1. Complex Synthesis

Na[Tn$^{t\mathrm{Bu}}$] was prepared according to literature procedures [12] and was subjected to a metathesis reaction with the respective zinc halides in dry dichloromethane to obtain complexes **1a** and **1b** as shown in Scheme 1.

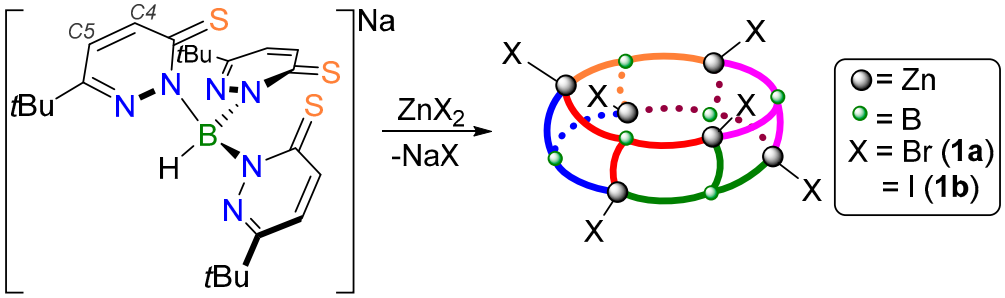

Scheme 1. Reaction of Na[Tn$^{t\mathrm{Bu}}$] with zinc halides to yield hexameric [Tn$^{t\mathrm{Bu}}$ZnX]$_6$ complexes (X = Br **1a**, I **1b**).

Because of the light sensitivity of the ligand [12], the syntheses of the complexes were conducted under exclusion of light. An excess of zinc salt was used in order to complete conversion of the ligand as otherwise unreacted Na[Tn$^{t\mathrm{Bu}}$] is difficult to remove. After reaction overnight and workup, the products were obtained as yellow powders in good yield (72–83%). In contrast to Na[Tn$^{t\mathrm{Bu}}$], **1a** and **1b** are not photo-reactive and are found to be stable under ambient atmosphere.

Characterization of the products in solution by ^{1}H and ^{13}C NMR spectroscopy revealed three sets of resonances for thiopyridazine substituents. Thus, the ^{1}H NMR spectrum of compound [Tn$^{t\mathrm{Bu}}$ZnBr]$_6$

(**1a**) in $CDCl_3$ shows six doublets between 8.83 and 7.03 ppm for the six aromatic thiopyridazine protons (Figure 1) and three singlets at 1.10, 1.04 and 0.91 ppm for the three *tert*-butyl groups. This asymmetric chemical surrounding within the scorpionate ligand is in contrast to a mononuclear [Tn$^{t\mathrm{Bu}}$ZnBr] complex with an expected C_3-symmetry, like in the case of the sodium salt of Tn$^{t\mathrm{Bu}}$, where only one set of resonance for all three thiopyridazine heterocycles is observed (Figure 1). Upon changing the halide from bromide in **1a** to iodide in **1b**, very similar spectra are observed with only the protons at C4 showing a slight downfield shift consistent with reduced electron density at zinc in the latter. The B–H atom is apparent at 5.88 ppm as a broad resonance for both complexes.

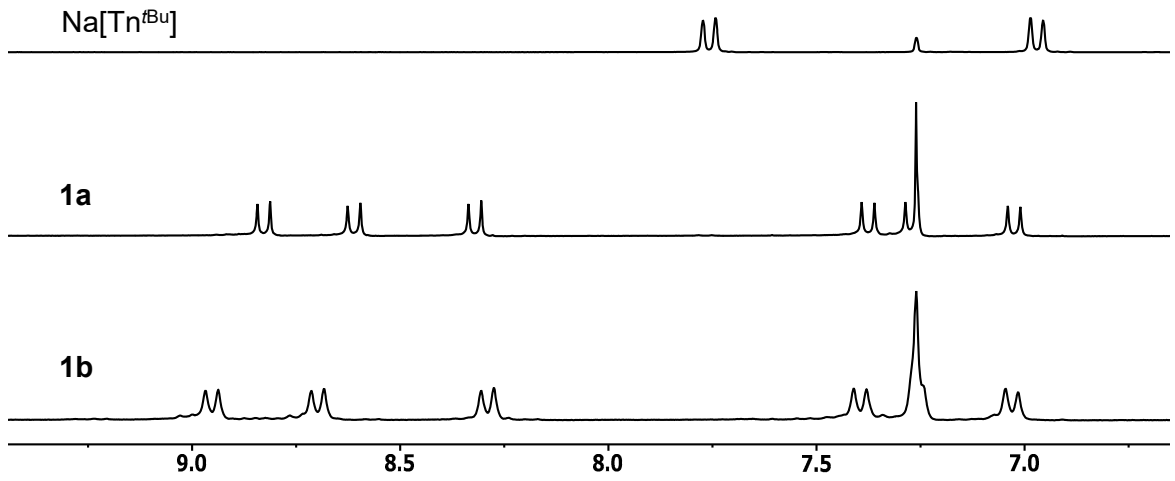

Figure 1. Aromatic region of the ^{1}H NMR spectra of Na[Tn$^{t\mathrm{Bu}}$] and the zinc complexes **1a** and **1b** in $CDCl_3$.

In addition, we consistently noticed a broad singlet integrating for two protons at 2.73 ppm for **1a** and 2.65 ppm for **1b**, respectively. This finding points towards the presence of one molecule of water in the products. The significant downfield shift compared to residual water in $CDCl_3$ (1.56 ppm) [24], indicates some sort of interaction with the zinc complexes. This is further supported by the observation that extensive drying for more than two days under reduced pressure (<0.05 mbar) did not remove the water molecule (increasing the temperature to 50 °C led to decomposition of the complexes). The source of water is as yet unclear, since all reactions were performed under inert atmosphere and in dry solvents. Possibly, our commercially available zinc halide starting materials were not dry enough.

By performing the preparation of **1a** and **1b** in tetrahydrofuran instead of methylene chloride, similar observations were made. The ^{1}H NMR spectra of the obtained solids revealed the same resonances, however, instead of the signal for H_2O, resonances for molecules of THF between one and two equiv were observed at 3.84 ppm and 1.89 ppm for **1a** and 3.96 ppm and 1.99 ppm for **1b**, respectively. Also in these complexes, extensive drying did not remove the THF molecules (again heating led to decomposition). A thermogravimetric analysis of **1a** showed a loss of mass of approximately 10 wt % up to 90 °C, in line with a loss of 2 equiv THF for this sample (see Supplementary Materials, Figure S16).

After dissolving these THF or water containing complexes **1a** and **2a** in dry chloroform, stirring for two days and subsequent solvent evaporation, powdery materials were obtained. Their characterization by ^{1}H NMR spectroscopy in dry $CDCl_3$ revealed again three sets of resonances for an asymmetric scorpionate ligand but any additional solvent molecules seemed to be absent. The resonances are slightly shifted to lower field compared to **1a** (especially of the C4 thiopyridazine protons: 8.96, 8.71 and 8.30 ppm vs. 8.83, 8.61 and 8.32 ppm in **1a**). We therefore conclude that the donor molecules H_2O or THF are displaced by the excess chloroform solvent molecules, which allows their removal by evaporation. Upon re-addition of THF to a chloroform solution of **1a**, ^{1}H NMR

spectra again show the presence of two coordinated THF molecules. Alternatively, pyridine—another excellent Lewis-basic donor molecule—can be added to solutions of **1a** and **1b**, also resulting in shifted ^{1}H NMR peaks (*vide infra*).

Single crystals of **1a** and **1b** could be obtained via slow diffusion of pentane into saturated $CHCl_3$ solutions. The molecular structure of **1a** and **1b**, as determined by single-crystal X-ray diffraction analysis (*vide infra*), revealed hexanuclear, cyclic arrangements (see Section 2.2), explaining the observed lack of symmetry in the recorded ^{1}H NMR spectra. We therefore reason that the hexanuclear structure is also preserved in solution. This raises the question of whether molecules might be trapped in the cavity. Such a situation could explain the observed shifted NMR signals of the donor molecules, but an interaction with the outside of the torus is also possible.

This was further investigated by diffusion-ordered ^{1}H NMR spectroscopy (DOSY) [25] of the crystalline compound $[Tn^{tBu}ZnBr]_6$ (**1a**). The DOSY experiment was performed with PPh_3 as internal standard, as PPh_3 would have a similar hydrodynamic radius compared to the mononuclear complex $[Tn^{tBu}ZnBr]$. After determination of the diffusion coefficient, the hydrodynamic radius was calculated according to the *Stokes-Einstein* equation (see Supplementary Materials, Figure S12, Equation 1) and the results are displayed in Table 1.

Table 1. Diffusion coefficient **D** and calculated hydrodynamic radius $\mathbf{R_H}$ of **1a** and PPh_3.

Compound	D (10^{-10} m^2/s)	R_H (Å)
1a	4.12	9.8
PPh_3	7.96	5.1

DOSY clearly reveals only one species in solution precluding a breaking of hexanuclear **1a** into lighter fragments. The smaller diffusion coefficient D found for **1a** compared to PPh_3 shows it to be significantly larger than a hypothetic monomer. This is supported by the calculated hydrodynamic radius for **1a** which was found to be 9.8 Å and thus in good agreement to the dimensions of the hexamer observed in the solid state (*vide infra*).

In order to gather information on the observed interaction with donor molecules, to a solution of $[Tn^{tBu}ZnBr]_6$ in $CDCl_3$, 2 equiv of pyridine were added ($Py_{(1a)}$). In this case, cyclooctene (COE) was used as internal standard, as there is a published value for the diffusion coefficient D available [26]. DOSY experiments of the mixture were performed and the diffusion coefficients were measured and referenced to COE. Furthermore, the diffusion coefficient of free pyridine was determined in an independent experiment (Figure 2).

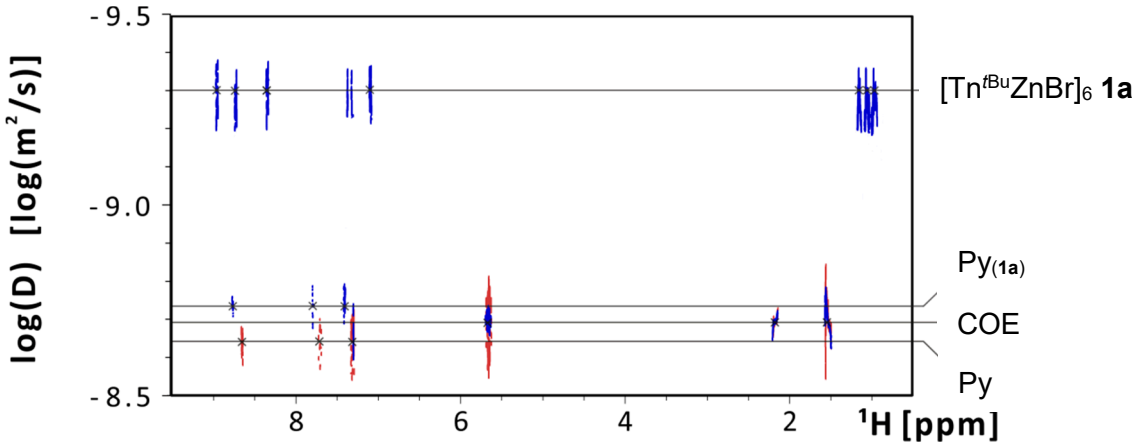

Figure 2. Diffusion ordered ^{1}H NMR spectroscopy (DOSY NMR) data of **1a**, the **1a+2pyridine** mixture ($Py_{(1a)}$, blue), free pyridine (Py, red) and cyclooctene (COE) as internal standard.

The DOSY NMR spectra (Figure S13, Supplementary Materials) of the **1a+2pyridine** mixture revealed two different diffusion coefficients D for the hexamer **1a** and the pyridine molecules, with the latter being higher. This provides evidence that the pyridine is not covalently bound to **1a** as it diffuses much faster. However, comparison of D of the pyridine in the mixture and of free pyridine from an independent experiment reveals a slightly lower diffusion coefficient (D = 19.1 $\times$ 10^{-10} m^2/s of the mixture **1a+2pyridine** vs. D = 24.5 $\times$ 10^{-10} m^2/s of free Py; Table S1, Supplementary Materials). The small difference, however, hints to only a weak interaction of pyridine with **1a**. Calculation of the diffusion partition coefficient (Equation 2 in Supplementary Materials) reveals that approximately 30% of the total pyridine in the mixture is on average interacting in a dynamic fashion. Nevertheless, from this data the assignment of the location (within or outside the cavity) cannot be determined.

While many coordination modes and applications for scorpionate complexes have been reported, the self-assembly of polynuclear zinc-frameworks is rare [27–31]. With soft scorpionates, only one tetranuclear [28] and one trinuclear complex [29] could be isolated, albeit in very low yield.

We wondered whether using a similar, but sterically more demanding, soft scorpionate ligand based on 4-methyl-6-*tert*-butyl-substituted thiopyridazines K[$Tn^{Me,tBu}$] will allow the isolation of a mononuclear zinc complex. However, application of the same reaction conditions used for the preparation of [Tn^{tBu}ZnX]$_6$ leads to decomposition of K[$Tn^{Me,tBu}$] with the only isolable product being Zn($HPn^{Me,tBu}$)$_2X_2$ (X = Br, **2a**; I, **2b**; Scheme 2). For complex **2a**, single crystals could be obtained, and the solid-state structure could be solved by single-crystal X-ray diffraction analysis (see Supplementary Materials).

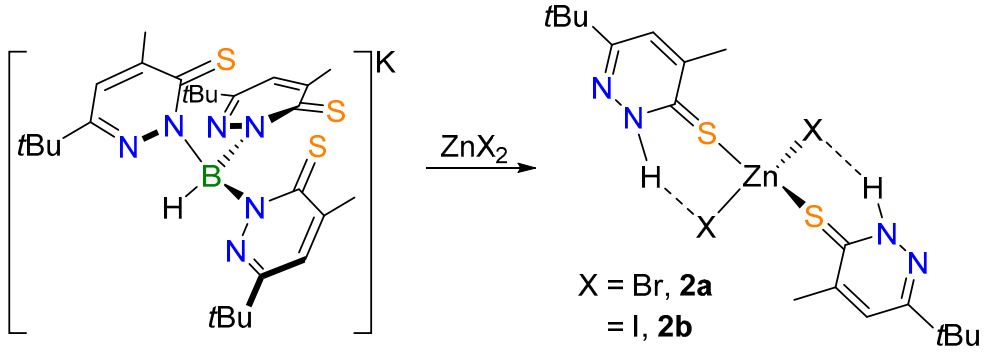

Scheme 2. Formation of Zn($HPn^{Me,tBu}$)$_2X_2$ (X = Br **2a**, I **2b**) upon reaction of K[$Tn^{Me,tBu}$] with zinc halides.

For unambiguous identification, **2a** and **2b** were synthesized independently by addition of 2 equiv of 4-methyl-6-*tert*-butyl-3-thiopyridazine ($HPn^{Me,tBu}$) to a stirred solution of the respective zinc halide allowing their isolation as light yellow powders in excellent yield (95–97%). The slightly reduced electrophilic nature of **2a**,**b** compared to the respective zinc halides led us to consider them as starting materials for the preparation of $Tn^{Me,tBu}$ complexes as decomposition of the latter might be suppressed. To prove this, the example of **2a** was used in the reaction with K[$Tn^{Me,tBu}$] in methylene chloride under exclusion of light to yield the mononuclear compound [$Tn^{Me,tBu}$]Zn($HPn^{Me,tBu}$)Br (**3**) as shown in Scheme 3.

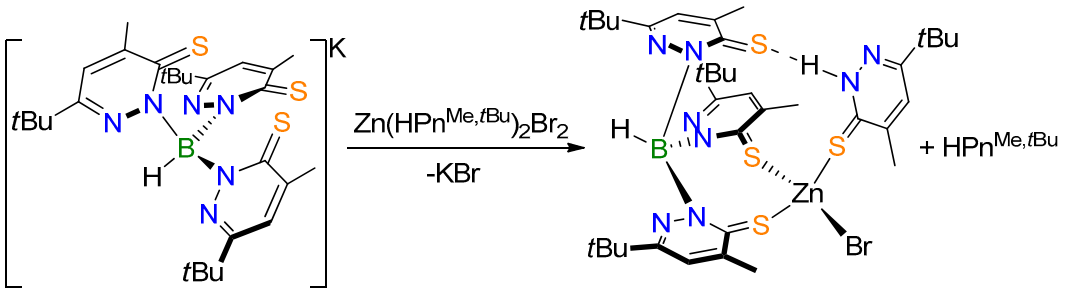

Scheme 3. Reaction of $Zn(HPn^{Me,tBu})_2Br_2$ (**2a**) with $K[Tn^{Me,tBu}]$ forming the mononuclear complex $[(Tn^{Me,tBu})Zn(HPn^{Me,tBu})Br]$ (**3**) and one equiv of $HPn^{Me,tBu}$.

The molecular structure of **3**, as determined by single-crystal X-ray diffraction analysis (*vide infra*), revealed a mononuclear compound coordinated by an intact $Tn^{Me,tBu}$ ligand, albeit only in the κ^2-S,S mode. For this reason, one molecule of $HPn^{Me,tBu}$ remains coordinated to Zn in order to conserve a tetrahedral geometry, while the second molecule of $HPn^{Me,tBu}$ of **2a** is released into solution. Although single crystals could be obtained, we were unable to isolate **3** in bulk, but in fact the 1:1 mixture of **3** and $HPn^{Me,tBu}$ was isolated in good yield (83%). Any attempt to separate the thiopyridazine from **3** by crystallization led to impure products. Furthermore, **3** shows limited stability in solution and decomposes within 24 h, both under ambient and inert atmosphere. Nevertheless, the isolated mixture **3**/$HPn^{Me,tBu}$ was subjected to ^{1}H NMR spectroscopy. The spectrum in $CDCl_3$ at room temperature revealed an unexpected, highly symmetric species in solution (Figure S10). No signals for free $HPn^{Me/tBu}$ were observed, indicating a fast, dynamic equilibrium between coordinated and uncoordinated $HPn^{Me/tBu}$. In the aliphatic region, only three broadened resonances for the five methyl (2.47 ppm; green peak in the r.t. spectrum, Figure 3) and *t*Bu-groups (1.22 and 0.99 ppm, blue and red peak in the r.t. spectrum, Figure 3) were observed, further pointing towards a dynamic behavior in solution. Indeed, by lowering the temperature to −50 °C, de-coalescence of all signals was observed (Figure S11). The signal at 0.99 ppm splits into three peaks of equal intensity, which is consistent with the non-symmetric solid state structure of **3**. In addition, signals for one equivalent of free $HPn^{Me,tBu}$ (2.45 and 1.30 ppm) [11] and one coordinated $HPn^{Me,tBu}$ moiety also appear (Figure 3). The observed dynamic behavior of **3** in solution at room temperature might explain its limited stability in solution.

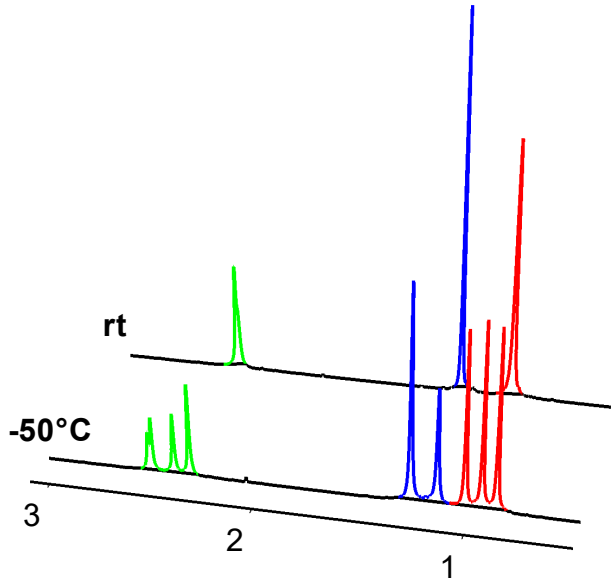

Figure 3. Aliphatic region of the ^{1}H NMR spectra of complex **3** at room temperature (top) and at −50 °C (bottom).

The observed different reactivity of $Tn^{Me,tBu}$ compared to the Tn^{tBu} ligand is fairly interesting. While the additional methyl group is certainly exhibiting both electronic and steric effects, we assume the former to be more pronounced. We have previously observed that the additional methyl group has little structural effect in the respective copper boratrane complexes [11]. However, the methyl substituted complexes are slightly better soluble and together with the increased donating properties, ligand substitution at the $Tn^{Me,tBu}$ zinc complexes might be facilitated, generating more dynamic and thus more labile systems.

2.2. Molecular Structures

Single crystals suitable for X-ray diffraction analysis of the complexes were obtained by slow diffusion of pentane (**1a**) or hexane (**1b**) into a chloroform solution or by slow evaporation of a chloroform solution (**3**). Compounds **1a** and **1b** were determined to be isostructural; however, the quality of the X-ray data of **1a** did not allow the discussion of structural details.

Compound **1b** was found to be of hexameric nature with six zinc iodide units coordinated by six scorpionate ligands (Figure 4). The complex forms a three-dimensional, cylindrical framework, where each thiopyridazine coordinates to a different zinc atom. While two arms of the scorpionate coordinate to two different zinc atoms in the same plane, the third thiopyridazine coordinates to a zinc atom on a different level.

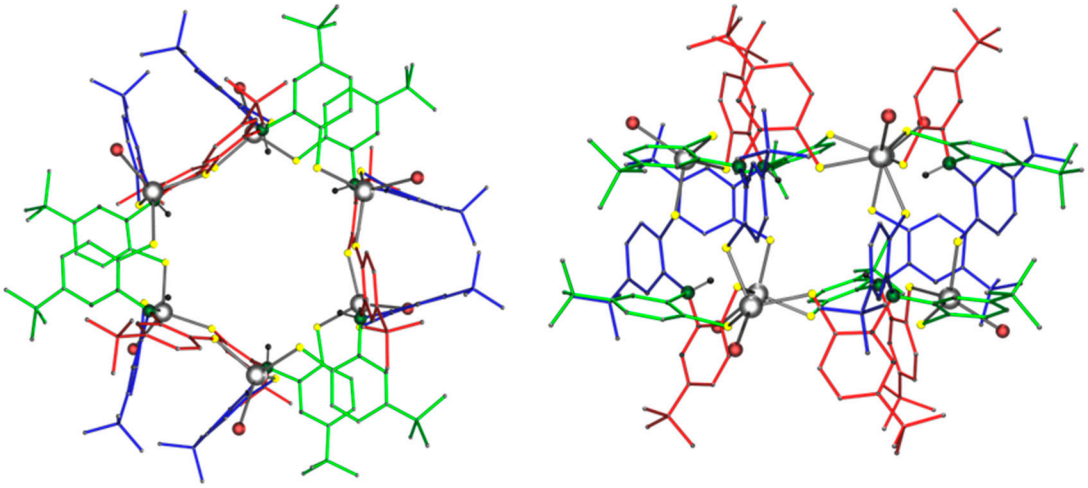

Figure 4. Molecular structure of **1b**. Left: view along the x-axis; right: view along the y-axis. Hydrogen atoms, except for those located at boron and disordered hexane solvent molecules, are omitted for clarity. Atom code: Zn gray, S yellow, B green, H black, I brown.

Each zinc center is coordinated by three sulfur donors from three different thiopyridazine ligands and by a halide atom leading to a distorted tetrahedral environment. This alternating coordination leads to the general framework displayed in Scheme 1. The dimension of the hexagon is approx. 20 Å in diameter and 12 Å in height, resulting in a volume of approximately 3800 $Å^3$. This is consistent with the determined hydrodynamic radius of 9.6 Å found by ^1H DOSY measurements.

The zinc-sulfur bond lengths (2.334–2.350 Å) are within the expected range of other sulfur coordinated zinc iodine scorpionate complexes (2.348–2.376 Å) [19,32–34]. In contrast, the zinc–iodine bonds (2.591–2.616 Å) are significantly longer than in other sulfur coordinated zinc iodine complexes (2.560 Å–2.580 Å) [19,32–34]. The only other example exhibiting similarly long Zn–I bonds represents the previously reported zinc–iodide containing tinsulfide cluster (2.605–2.611 Å) [35].

The structure also reveals a cavity which is approximately 8 Å wide and 6 Å deep and with a volume of approximately 300 $Å^3$ shielded by the *tert*-butyl groups of the ligands (Figure 5). This is very similar to the dimensions of cucurbit[6]uril (CB[6]), a macrocyclic cavitand comprising of six glycoluril units forming a cavity which is 5.5 Å wide and 6 Å high [36,37]. Applications of CB[6] are

manifold including catalytic processes, molecular recognition with highly selective binding interactions, waste-water remediation, or as artificial enzymes or molecular switches [38]. Thus, the observation of the donor molecule interaction properties of complex **1a**, as described above, are interesting as **1a** and **1b** might show potential for similar applications with the right choice of guest molecules.

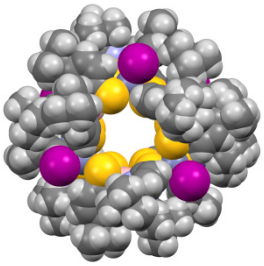

Figure 5. Space filling representation of **1b**.

The solid-state structure is consistent with the asymmetric nature observed by ^{1}H and ^{13}C NMR spectroscopy supporting the stability of the hexameric structure in solution. Thus, the C_3 axis running through the torus reveals three thiopyridazine rings that differ in their relative orientation: two thiopyridazine rings in the plane, that are perpendicular to each other, and one ring which is perpendicular to the plane (Figure 4). This results in three different thiopyridazines as observed by NMR spectroscopy.

Details regarding the solid-state structure and data refinement of **2a** can be found in the supporting information (Figure S20, Table S4). The molecular structure of **3** is displayed in Figure 6. It reveals a mononuclear zinc complex, coordinated by the $Tn^{Me,tBu}$ ligand in a κ^2-S,S fashion, a bromine and a sulfur atom from an additional thiopyridazine molecule. Furthermore, interaction between the borohydride and the zinc center is evidenced by the relatively short Zn1–H1 distance of 2.45(5) Å, the almost linear H1–Zn1–Br1 angle (175.2(12)°) and the distortion from a tetrahedral to a distorted trigonal bipyramidal coordination at zinc (Br1–Zn1–S1 102.51(8)°, Br1–Zn1–S2 95.75(7)°, Br1–Zn1–S4 105.47(8)°). The $HPn^{Me,tBu}$ molecule is further stabilized by hydrogen bonding to the sulfur atom of the non-coordinating arm of the scorpionate ligand (S3–H42 2.322(10) Å).

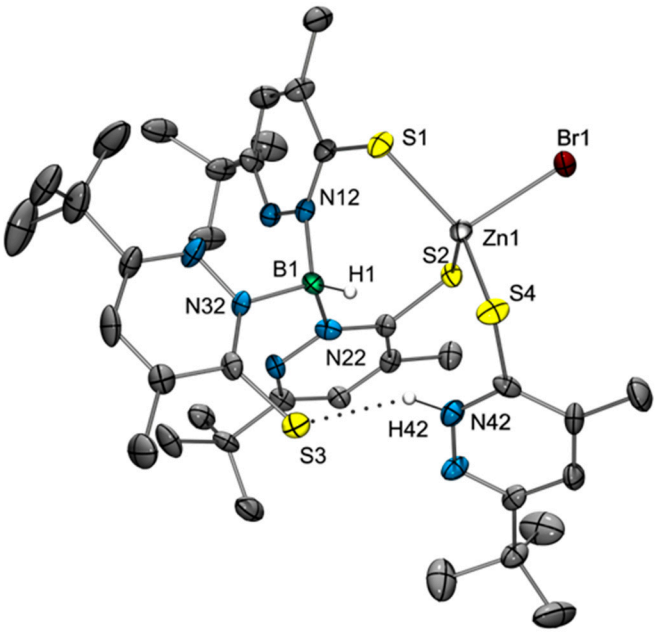

Figure 6. Molecular structure of $[Tn^{Me,tBu}]Zn(HPn^{Me,tBu})Br$ (**3**). Hydrogen atoms, except for those on B1 and N42, as well as solvent molecules are omitted for clarity. Hydrogen bonding is depicted in dashed lines.

Compared to zinc bromide complexes coordinated by various methimazolyl-based scorpionate ligands, the Zn1–Br1 bond with a length of 2.4250(13) Å is significantly elongated (2.334 Å–2.372 Å) [9,39,40]. This might be due to the additional B–H–Zn interaction, because the Zn–Br bond lengths in **2a** (2.41252(18) Å and 2.38838(18) Å) as well as in the hybrid methimazolyl-thiopyridazinyl based dinuclear $[(^{Pn}Bm)ZnBr]_2$ zinc scorpionate complex (2.409 Å) are in the same range as in **3** [21].

3. Experimental Section

3.1. General Information

All reactions were carried out using standard Schlenk techniques. 6-*tert*-butyl-3-thiopyridazine (HPn^{tBu}), 4-methyl-6-*tert*-butyl-3-thiopyridazine ($HPn^{Me,tBu}$), $Na[Tn^{tBu}]$ and $K[Tn^{Me,tBu}]$ were synthesized according to literature procedures [11,12,41]. NMR spectra, except for the DOSY experiments, were measured with a Bruker Avance III 300 MHz spectrometer (Bruker, Billerica, MA, USA) at 25 °C. DOSY experiments were carried out at 300 K on a 500 MHz Bruker Avance III spectrometer, equipped with a 5 mm TXI probe with z-gradient. To measure the diffusion coefficients, bipolar pulse pair longitudinal eddy current delay sequences (BPP-LED) [42] were used together with an additional convection compensation sequence (double stimulated echo BPP-LED) [43,44]. The diffusion time Δ was 30 ms and the spoil gradient δ was 1 ms. High resolution mass spectrometry was measured at the University of Technology of Graz, using a Waters GCT Premier Micromas MS Technologies mass spectrometer (Waters, Milfird, MA, USA) with DI-EI and a TOF detector.

X-ray Structure Determinations were performed with a Bruker AXS SMART APEX 2 CCD diffractometer (Bruker, Billerica, MA, USA) equipped with an Incoatec microfocus sealed tube and a multilayer monochromator (Mo Kα, 0.71073 Å) at 100 K. The structures were solved by direct methods (*SHELXS*-97) [45] and refined by full-matrix least-squares techniques against F^2 (*SHELXL*-2014/6) [45]. The non-hydrogen atoms were refined with anisotropic displacement parameters without any constraints. The H atoms bonded to the B atoms could be clearly identified in a difference Fourier map and were refined with a common isotropic displacement parameter. H atoms bonded to N atoms could be clearly identified in a difference Fourier map, the N–H distances were fixed to 0.88 Å and refined without constraints to the bond angles. The H atoms of the pyridazine rings were put at the external bisectors of the C–C–C angles at C–H distances of 0.95 Å and a common isotropic displacement parameter was refined for the H atoms of the same ring. The H atoms of the *tert*-butyl groups were included at calculated positions with their isotropic displacement parameter fixed to 1.1 times U_{eq} of the C atom they are bonded to and idealized geometries with tetrahedral angles, staggered conformations, and C–H distances of 0.98 Å.

CCDC 1510468 (**1b**), 1850650 (**2a**) and 1850650 (**3**) contain the supplementary crystallographic data for this paper. These data can be obtained free of charge via http://www.ccdc.cam.ac.uk/conts/retrieving.html (or from the CCDC, 12 Union Road, Cambridge CB2 1EZ, UK; Fax: +44 1223 336033; E-mail: deposit@ccdc.cam.ac.uk).

3.2. Synthetic Procedures

$[Tn^{tBu}ZnBr]_6$ (1a). Under exclusion of light, 200 mg (0.37 mmol, 1.0 equiv) of $Na[Tn^{tBu}]$ and 125 mg (0.56 mmol, 1.5 equiv) of $ZnBr_2$ were suspended in 5 mL of methylene chloride and the beige suspension was stirred for 16 h. Thereafter, the insoluble parts were removed by filtration and the yellow solution was dried in vacuo. The crude product was washed with 2× 10 mL of pentane and dried in vacuo to obtain 210 mg (83%) of **1a**·H_2O as a light yellow powder. ^{1}H NMR ($CDCl_3$) δ (ppm): 8.83 (d, *J* = 9.3 Hz, 1H, ArH), 8.61 (d, *J* = 9.0 Hz, 1H, ArH), 8.32 (d, *J* = 9.3 Hz, 1H, ArH), 7.38 (d, *J* = 9.3 Hz, 1H, ArH), 7.27 (d, *J* = 9.0 Hz, 1H, ArH), 7.03 (d, *J* = 9.3 Hz, 1H, ArH), 5.88 (bs, 1H, BH), 2.73 (bs, 2H, H_2O), 1.10 (s, 9H, *t*Bu), 1.04 (s, 9H, *t*Bu), 0.91 (s, 9H, *t*Bu). ^{13}C NMR ($CDCl_3$) δ (ppm): 175.71 (Ar-**C**), 174.76 (Ar-**C**), 173.48 (Ar-**C**), 163.31 (Ar-**C**), 162.80 (Ar-**C**), 162.53 (Ar-**C**), 140.58 (Ar-**C**), 139.83 (Ar-**C**), 138.31 (Ar-**C**), 125.11 (Ar-**C**), 124.38 (Ar-**C**), 123.94 (Ar-**C**), 36.69 (2× *t*Bu-**C**), 36.63 (*t*Bu-**C**), 29.06

(*t*Bu-**C**CH_3), 29.03 (*t*Bu-**C**CH_3), 28.90 (*t*Bu-**C**CH_3). MALDI-HR-MS: $[Zn_2Tn_2Br]^+$ calc: 1237.194 m/z, found: 1237.199 m/z, $[Zn_4Tn_4I_4Na]^+$ calc: 2658.21 m/z, found: 2657.20 m/z; no peaks for the hexanuclear molecular ion could be detected. Crystals suitable for X-ray diffraction analysis were obtained by slow diffusion of pentane into a chloroform solution.

A sample of **1a** was dissolved in $CDCl_3$ in a Young tube and stored for 2 days at room temperature. After the yellow solution has turned slightly bluish, the solvent was removed under reduced pressure, to obtain **1a** without additional H_2O as a slightly bluish powder. Recrystallization from $CDCl_3$ and pentane yielded slightly blue plates. ^{1}H NMR ($CDCl_3$) δ (ppm): 8.96 (d, *J* = 9.3 Hz, 1H, ArH), 8.71 (d, *J* = 9.0 Hz, 1H, ArH), 8.30 (d, *J* = 9.3 Hz, 1H, ArH), 7.40 (d, *J* = 9.3 Hz, 1H, ArH), 7.26 (d, *J* = 9.0Hz, 1H, ArH), 7.04 (d, *J* = 9.3 Hz, 1H, ArH), 5.88 (bs, 1H, BH), 1.13 (s, 9H, *t*Bu), 1.05 (s, 9H, *t*Bu), 0.93 (s, 9H, *t*Bu). ^{13}C NMR ($CDCl_3$) δ (ppm): 175.71 (Ar-**C**), 174.76 (Ar-**C**), 173.48 (Ar-**C**), 163.31 (Ar-**C**), 162.80 (Ar-**C**), 162.53 (Ar-**C**), 140.58 (Ar-**C**), 139.83 (Ar-**C**), 138.31 (Ar-**C**), 125.11 (Ar-**C**), 124.38 (Ar-**C**), 123.94 (Ar-**C**), 36.69 (*t*Bu-**C**), 36.63 (*t*Bu-**C**), 29.06 (*t*Bu-**C**CH_3), 29.03 (*t*Bu-**C**CH_3), 28.90 (*t*Bu-**C**CH_3).

$[Tn^{tBu}ZnI]_6$ (1b). Under inert atmosphere and light exclusion, 200 mg (1.0 equiv 0.37 mmol) of Na[Tn^{tBu}] and 190 mg (1.5 equiv 0.56 mmol) ZnI_2 were suspended in 5 mL of dry methylene chloride and the beige suspension was stirred for 16 h. Thereafter, the insoluble salts were removed by filtration and the yellow solution was dried in vacuo. The crude product was washed with 2× 10 mL of dry pentane and dried in vacuo to obtain 195 mg (72%) of **1b**·H_2O as a light yellow powder. ^{1}H NMR ($CDCl_3$) δ (ppm) 8.96 (d, *J* = 9.1 Hz, 1H, ArH), 8.70 (d, *J* = 9.1 Hz, 1H, ArH), 8.29 (d, *J* = 9.2 Hz, 1H, ArH), 7.40 (d, *J* = 9.2 Hz, 1H, ArH), 7.26 (bd, 1H, ArH), 7.04 (d, *J* = 9.1 Hz, 1H, ArH), 5.88 (bs, 1H, BH), 2.65 (bs, 2H, H_2O), 1.12 (s, 9H, *t*Bu), 1.05 (s, 9H, *t*Bu), 0.92 (s, 9H, *t*Bu). ^{13}C NMR ($CDCl_3$) δ (ppm): 175.73 (Ar-**C**), 174.82 (Ar-**C**), 173.23 (Ar-**C**), 163.26 (Ar-**C**), 162.99 (Ar-**C**), 162.59 (Ar-**C**), 140.92 (Ar-**C**), 138.89 (Ar-**C**), 137.53 (Ar-**C**), 124.98 (Ar-**C**), 124.18 (Ar-**C**), 123.98 (Ar-**C**), 36.85 (*t*Bu-**C**), 36.67 (*t*Bu-**C**), 36.64 (*t*Bu-**C**), 29.16 (*t*Bu-**C**CH_3), 29.08 (*t*Bu-**C**CH_3), 28.94 (*t*Bu-**C**CH_3). MALDI-HR-MS: $[Zn_2Tn_2I]^+$ calc: 1285.180 m/z, found: 1285.187 m/z, no peaks for the hexanuclear molecular ion could be detected. Crystals suitable for X-ray diffraction analysis were obtained by slow diffusion of hexane into a chloroform solution.

A sample of **1b** was dissolved in $CDCl_3$ in a Young tube and stored for 2 days at room temperature. After the yellow solution has turned slightly bluish, the solvent was removed under reduced pressure, to obtain H_2O free **1b** as a bluish powder. ^{1}H NMR ($CDCl_3$) δ (ppm) 8.95 (d, *J* = 9.1 Hz, 1H, ArH), 8.70 (d, *J* = 9.1 Hz, 1H, ArH), 8.29 (d, *J* = 9.2 Hz, 1H, ArH), 7.40 (d, *J* = 9.2 Hz, 1H, ArH), 7.26 (d, *J* = 9.2 Hz, 1H, ArH), 7.03 (d, *J* = 9.1 Hz, 1H, ArH), 5.88 (bs, 1H, BH), 1.12 (s, 9H, *t*Bu), 1.05 (s, 9H, *t*Bu), 0.92 (s, 9H, *t*Bu). ^{13}C NMR ($CDCl_3$) δ (ppm): 175.73 (Ar-**C**), 174.82 (Ar-**C**), 173.23 (Ar-**C**), 163.26 (Ar-**C**), 162.99 (Ar-**C**), 162.59 (Ar-**C**), 140.92 (Ar-**C**), 138.89 (Ar-**C**), 137.53 (Ar-**C**), 124.98 (Ar-**C**), 124.18 (Ar-**C**), 123.98 (Ar-**C**), 36.85 (*t*Bu-**C**), 36.67 (*t*Bu-**C**), 36.64 (*t*Bu-**C**), 29.16 (*t*Bu-**C**CH_3), 29.08 (*t*Bu-**C**CH_3), 28.94 (*t*Bu-**C**CH_3).

$Zn(HPn^{Me,tBu})_2Br_2$ (2a). $ZnBr_2$ (50 mg, 0.222 mmol) and $HPn^{Me,tBu}$ (81 mg, 0.444 mmol) were dissolved in 3 mL of dichloromethane and the resulting solution was stirred under inert conditions and exclusion of light overnight. Subsequently, all volatiles were removed *in vacuo*, the crude product was washed with 5 mL of pentane and dried to obtain a light yellow powder of **2a** (127 mg, 97%). ^{1}H NMR ($CDCl_3$) δ 14.28 (bs, 2H, NH), 7.46 (d, 2H, ArH), 2.47 (d, 6H, Me), 1.35 (s, 18H, *t*Bu); ^{13}C NMR ($CDCl_3$) δ 172.37 (Ar-**C**), 164.85 (Ar-**C**), 148.75 (Ar-**C**), 127.46 (Ar-**C**), 36.84 (*t*Bu-**C**CH_3), 29.20 (*t*Bu-**C**), 20.69 (Me-**C**). Anal. calcd. for $C_{18}H_{28}Br_2N_4S_2Zn$ (589.76): C: 36.66, H: 4.79, N: 9.50, S: 10.87; found C: 36.84, H: 4.78, N: 9.24, S: 10.41. Single crystals suitable for X-ray diffraction measurement were obtained by slow evaporation of a $CHCl_3$ solution.

$Zn(HPn^{Me,tBu})_2I_2$ (2b). ZnI_2 (44 mg, 0.137 mmol) and 2 equiv of $HPn^{Me,tBu}$ (50 mg, 0.274 mmol) were dissolved in 3 mL of dichloromethane and the resulting solution was stirred under inert conditions and exclusion of light overnight. Subsequently, all volatiles were removed *in vacuo*, the crude product was washed with 5 mL of pentane and dried to obtain a light yellow powder of **2b** (89 mg, 95%). ^{1}H NMR ($CDCl_3$) δ 13.48 (bs, 2H, NH), 7.43 (d, 2H, ArH), 2.46 (d, 6H, Me), 1.35 (s, 18H, *t*Bu); ^{13}C NMR ($CDCl_3$) δ 164.52 (Ar-**C**), 149.13 (Ar-**C**), 127.05 (Ar-**C**), 36.86 (*t*Bu-**C**CH_3), 29.22 (*t*Bu-**C**), 20.80 (Me-**C**).

Anal. calcd. for $C_{18}H_{28}I_2N_4S_2Zn$ (683.76): C: 31.62, H: 4.13, N: 8.19, S: 9.38; found C: 33.52, H: 4.36, N: 8.66, S: 9.83.

[Tn^{Me,tBu}]Zn(HPn^{Me,tBu})Br (3). K[Tn^{Me,tBu}] (326 mg, 0.549 mmol) was dissolved under exclusion of light in 8 mL of dichloromethane. Subsequently, **2a** (324 mg, 0.549 mmol) was added to the yellow solution. The reaction mixture was stirred in the dark for 5 h after which the formed precipitate was filtered off and the solvent evaporated. The crude material was washed with 5 mL of pentane and dried *in vacuo* to obtain 480 mg (82%) of **3·HPn^{Me,tBu}** as a light yellow solid. ^{1}H NMR ($CDCl_3$) δ 13.09 (bs, 2H, NH of HPn^{Me,tBu}), 7.28 (s, 3H, ArH of **3**), 7.19 (s, 2H, ArH of HPn^{Me,tBu}), 6.91 (bs, 1H, B–H of **3**), 2.47 (bs, 15H, Me), 1.26 (bs) and 0.99 (bs, 45H, *t*Bu). Due to the dynamic behavior of the complex, no ^{13}C NMR data could be obtained. Anal. calc. of $C_{36}H_{54}BBrN_8S_4Zn{\cdot}C_9H_{14}N_2S$: calc: C: 50.73, H: 6.43, N: 13.15, S: 15.04; found C: 50.32, H: 6.28, N: 13.03, S: 14.77. Single crystals suitable for X-ray diffraction measurement were obtained by slow evaporation of a $CHCl_3$ solution.

4. Conclusions

Herein we present the high yield synthesis of neutral, three-dimensional, hexanuclear zinc complexes that derive from hydrotris-(6-*tert*-butyl-3-thiopyridazinyl)borate. The complexes display the first structurally characterized zinc dependent molecular cage with a scorpionate ligand. ^{1}H DOSY NMR measurements confirmed only one species in solution and revealed a hydrodynamic radius of 9.8 Å, which is consistent with the dimensions observed in the solid state structure as determined by single crystal X-ray diffraction analysis. The molecular structure reveals a torus with an 8 Å wide and 6 Å deep cavity that is surrounded by *tert*-butyl groups. Residual electron density in- and outside of the hexameric structure points to large amounts of solvent molecules which could however not be further resolved (also see Supplementary Materials). These solvent molecules can be exchanged by polar molecules such as water, tetrahydrofuran or pyridine. Based on ^{1}H DOSY experiments they are not covalently bound to the hexamer. Although only weakly bound—presumably by van-der-Waals forces—they cannot be removed from the solid material by evaporation. This is also consistent with the properties of the cucurbit[n]uril family (CB[n]) which act as host-guest materials [38]. The cavity of the best-studied congener CB[6] has very similar dimensions to those of the hexameric zinc species **1b** rendering the latter a potential host material. Although likely, with the data in hand we cannot conclusively state whether the "guest" molecules are indeed inside the cavity in our hexamers.

Increased steric demand on the scorpionate ligand leads under the same reaction conditions predominantly to decomposition of the ligand under formation of Zn(HPn^{Me,tBu})$_2$X$_2$. However, using the latter (X = Br) as precursor allows for the isolation of a monomeric zinc scorpionate complex in which the zinc center is coordinated by the scorpionate ligand in the κ^2-S,S mode and additionally by a protonated thiopyridazine molecule and bromine, as confirmed by single-crystal X-ray diffraction analysis. Furthermore, these data showcase a short Zn–H distance within an almost linear Zn–H–B interaction. Low temperature ^{1}H NMR spectroscopy is consistent with the solid state structure, while at room temperature dynamic behavior was observed, possibly explaining the limited stability the methyl substituted system.

This research shows that the thiopyridazine based scorpionate ligands [Tn^{tBu}] and [Tn^{Me,tBu}] can coordinate to zinc centers, albeit they do not form mononuclear species of the formula [Tn^R]ZnX. Although the additional methyl group in [Tn^{Me,tBu}] prevents formation of a polynuclear framework, the resulting Lewis acidity of the zinc center leads to decomposition of the ligand, forming the less acidic Zn(HPn^{Me,tBu})$_2$X$_2$. The usage of this precursor circumvents the problem of increased Lewis acidity, but the formed product cannot be properly purified and decomposes after prolonged time in solution.

Supplementary Materials: The following are available online at http://www.mdpi.com/2304-6740/7/2/24/s1: NMR spectra of all compounds, Thermogravimetric analysis of **1a** and crystallographic details.

Author Contributions: For research articles with several authors, a short paragraph specifying their individual contributions must be provided. Conceptualization, N.C.M.-Z.; synthetic experiments, M.T. and M.R.; DOSY

experiments, S.G. and K.Z.; X-ray analysis, F.B.; writing—original draft preparation, M.T.; writing—review and editing, contributions of all authors visualization; supervision, N.C.M.-Z.

Acknowledgments: Support from NAWI Graz is gratefully acknowledged.

Conflicts of Interest: The authors declare no conflict of interest.

References

1. Trofimenko, S. Scorpionates: Genesis, milestones, prognosis. *Polyhedron* **2004**, *23*, 197–203. [CrossRef]
2. Trofimenko, S. Boron-Pyrazole Chemistry. *J. Am. Chem. Soc.* **1966**, *3*, 1842–1844. [CrossRef]
3. Trofimenko, S. Recent Advances in Poly(pyrazoly1) borate (Scorpionate) Chemistry. *Chem. Rev.* **1993**, *93*, 943–980. [CrossRef]
4. Parkin, G. Synthetic analogues relevant to the structure and function of zinc enzymes. *Chem. Rev.* **2004**, *104*, 699–767. [CrossRef]
5. Costas, M.; Chen, K.; Que, L. Biomimetic nonheme iron catalysts for alkane hydroxylation. *Coord. Chem. Rev.* **2000**, *202*, 517–544.
6. Spicer, M.D.; Reglinski, J. Soft Scorpionate Ligands Based on Imidazole-2-thione Donors. *Eur. J. Inorg. Chem.* **2009**, *2009*, 1553–1574. [CrossRef]
7. Dyson, G.; Hamilton, A.; Mitchell, B.; Owen, G.R. A new family of flexible scorpionate ligands based on 2-mercaptopyridine. *Dalton Trans.* **2009**, 6120. [CrossRef]
8. Nuss, G.; Saischek, G.; Harum, B.N.; Volpe, M.; Gatterer, K.; Belaj, F.; Mösch-Zanetti, N.C. Novel pyridazine based scorpionate ligands in cobalt and nickel boratrane compounds. *Inorg. Chem.* **2011**, *50*, 1991–2001. [CrossRef] [PubMed]
9. Garner, M.; Reglinski, J.; Cassidy, I.; Spicer, M.D.; Kennedy, A.R. Hydrotris(methimazolyl)borate, a soft analogue of hydrotris(pyrazolyl)borate. Preparation and crystal structure of a novel zinc complex. *Chem. Commun.* **1996**, *355*, 1975–1976. [CrossRef]
10. Nuss, G.; Saischek, G.; Harum, B.N.; Volpe, M.; Belaj, F.; Mösch-Zanetti, N.C. Pyridazine based scorpionate ligand in a copper boratrane compound. *Inorg. Chem.* **2011**, *50*, 12632–12640. [CrossRef] [PubMed]
11. Holler, S.; Tüchler, M.; Belaj, F.; Veiros, L.F.; Kirchner, K.; Mösch-Zanetti, N.C. Thiopyridazine-Based Copper Boratrane Complexes Demonstrating the Z-type Nature of the Ligand. *Inorg. Chem.* **2016**, *55*, 4980–4991. [CrossRef]
12. Tüchler, M.; Belaj, F.; Raber, G.; Neshchadin, D.; Mösch-Zanetti, N.C. Photoinduced Reactivity of the Soft Hydrotris(6-tert-butyl-3-thiopyridazinyl)borate Scorpionate Ligand in Sodium, Potassium, and Thallium Salts. *Inorg. Chem.* **2015**, *54*, 8168–8170. [CrossRef] [PubMed]
13. Tüchler, M.; Holler, S.; Schachner, J.A.; Belaj, F.; Mösch-Zanetti, N.C. Unusual C–N Coupling Reactivity of Thiopyridazines: Efficient Synthesis of Iron Diorganotrisulfide Complexes. *Inorg. Chem.* **2017**, *56*, 8159–8165. [CrossRef]
14. Parkin, G. The bioinorganic chemistry of zinc: Synthetic analogues of zinc enzymes that feature tripodal ligands. *Chem. Commun.* **2000**, 1971–1985. [CrossRef]
15. Sattler, W.; Parkin, G. Structural characterization of zinc bicarbonate compounds relevant to the mechanism of action of carbonic anhydrase. *Chem. Sci.* **2012**, *3*, 2015–2019. [CrossRef]
16. Alsfasser, R.; Trofimenko, S.; Looney, A.G.; Parkin, G.; Vahrenkamp, H. A mononuclear zinc hydroxide complex stabilized by a highly substituted tris(pyrazolyl)hydroborato ligand: Analogies with the enzyme carbonic anhydrase. *Inorg. Chem.* **1991**, *30*, 4098–4100. [CrossRef]
17. Looney, A.G.; Han, R.; Mcneill, K.; Parkin, G. Tris (pyrazolyl) hydroboratozinc Hydroxide Complexes as Functional Models for Carbonic Anhydrase: On the Nature of the Bicarbonate Intermediate. *J. Am. Chem. Soc.* **1993**, *115*, 4690–4697. [CrossRef]
18. Bridgewater, B.M.; Parkin, G. A zinc hydroxide complex of relevance to 5-aminolevulinate dehydratase: The synthesis, structure and reactivity of the *tris*(2-mercapto-1-phenylimidazolyl) hydroborato complex [Tm^{Ph}]ZnOH. *Inorg. Chem. Commun.* **2001**, *4*, 126–129. [CrossRef]
19. Kimblin, C.; Bridgewater, B.M.; Churchill, D.G.; Parkin, G. Mononuclear *tris*(2-mercapto-1-arylimidazolyl) hydroborato complexes of zinc, [Tm^{Ar}]ZnX: Structural evidence that a sulfur rich coordination environment promotes the formation of a tetrahedral alcohol complex in a synthetic analogue of LADH. *Chem. Commun.* **1999**, *993*, 2301–2302. [CrossRef]

20. Ibrahim, M.M.; Olmo, C.P.; Tekeste, T.; Seebacher, J.; He, G.; Maldonado Calvo, J.A.; Böhmerle, K.; Steinfeld, G.; Brombacher, H.; Vahrenkamp, H. Zn–OH_2 and Zn–OH Complexes with Hydroborate-Derived Tripod Ligands: A Comprehensive Study. *Inorg. Chem.* **2006**, *45*, 7493–7502. [CrossRef]
21. Tüchler, M.; Holler, S.; Huber, E.; Fischer, S.; Boese, A.D.; Belaj, F.; Mösch-Zanetti, N.C. Synthesis and Characterization of a Thiopyridazinylmethane-Based Scorpionate Ligand: Formation of Zinc Complexes and Rearrangement Reaction. *Organometallics* **2017**, *36*, 3790–3798. [CrossRef]
22. Tüchler, M.; Gärtner, L.; Fischer, S.; Boese, A.D.; Belaj, F.; Mösch-Zanetti, N.C. Efficient CO_2 Insertion and Reduction Catalyzed by a Terminal Zinc Hydride Complex. *Angew. Chem. Int. Ed.* **2018**, *57*, 6906–6909. [CrossRef] [PubMed]
23. Tüchler, M.; Holler, S.; Rendl, S.; Stock, N.; Belaj, F.; Mösch-Zanetti, N.C. Zinc Scorpionate Complexes with a Hybrid (Thiopyridazinyl)(thiomethimidazolyl)borate Ligand. *Eur. J. Inorg. Chem.* **2016**, *2016*, 2609–2614. [CrossRef]
24. Fulmer, G.R.; Miller, A.J.M.; Sherden, N.H.; Gottlieb, H.E.; Nudelman, A.; Stoltz, B.M.; Bercaw, J.E.; Goldberg, K.I. NMR Chemical Shifts of Trace Impurities: Common Laboratory Solvents, Organics, and Gases in Deuterated Solvents Relevant to the Organometallic Chemist. *Organometallics* **2010**, *29*, 2176–2179. [CrossRef]
25. Gibbs, S.J.; Johnson, C.S. A PFG NMR experiment for accurate diffusion and flow studies in the presence of eddy currents. *J. Magn. Reson.* **1991**, *93*, 395–402. [CrossRef]
26. Li, D.; Kagan, G.; Hopson, R.; Williard, P.G. Formula weight prediction by internal reference diffusion-ordered NMR spectroscopy (DOSY). *J. Am. Chem. Soc.* **2009**, *131*, 5627–5634. [CrossRef] [PubMed]
27. Parkin, G. Applications of Tripodal [S_3] and [Se_3] L_2X Donor Ligands to Zinc, Cadmium and Mercury Chemistry: Organometallic and Bioinorganic Perspectives. *New J. Chem.* **2007**, *31*, 1996–2014. [CrossRef]
28. Seebacher, J.; Vahrenkamp, H. A new bonding mode of tripodal sulfur ligands: Synthesis and structure of tetranuclear [$Tt^{t\text{-}Bu}$Zn]ClO_4. *J. Mol. Struct.* **2003**, *656*, 177–181. [CrossRef]
29. Schneider, A.; Vahrenkamp, H. Ein dreikerniger Zinkkomplex mit ZnS_4-, ZnS_3O- und ZnS_2NO-Koordinationen. *Z. Anorg. Allg. Chem.* **2004**, *630*, 1059–1061. [CrossRef]
30. Paul, R.L.; Amoroso, A.J.; Jones, P.L.; Couchman, S.M.; Reeves, Z.R.; Rees, L.H.; Jeffery, J.C.; McCleverty, J.A.; Ward, M.D. Effects of metal co-ordination geometry on self-assembly: A monomeric complex with trigonal prismatic metal co-ordination vs. tetrameric complexes with octahedral metal co-ordination. *J. Chem. Soc. Dalton Trans.* **1999**, 1563–1568. [CrossRef]
31. Zhang, D.-X.; Zhang, H.-X.; Wen, T.; Zhang, J. Targeted design of a cubic boron imidazolate cage with sensing and reducing functions. *Dalton Trans.* **2015**, *44*, 9367–9369. [CrossRef]
32. Cassidy, I.; Garner, M.; Kennedy, A.R.; Potts, G.B.S.; Reglinski, J.; Slavin, P.A.; Spicer, M.D. The Preparation and Structures of Group 12 (Zn, Cd, Hg) Complexes of the Soft Tripodal Ligand Hydrotris(methimazolyl)borate (Tm). *Eur. J. Inorg. Chem.* **2002**, *2002*, 1235–1239. [CrossRef]
33. Yurkerwich, K.; Yurkerwich, M.; Parkin, G. Synthesis and structural characterization of tris(2-mercapto-1-adamantylimidazolyl)hydroborato complexes: A sterically demanding tripodal [S_3] donor ligand. *Inorg. Chem.* **2011**, *50*, 12284–12295. [CrossRef] [PubMed]
34. Melnick, J.G.; Docrat, A.; Parkin, G. Methyl, hydrochalcogenido, and phenylchalcogenolate complexes of zinc in a sulfur rich coordination environment: Syntheses and structural characterization of the tris(2-mercapto-1-tert-butylimidazolyl)hydroboratozinc complexes [Tm^{But}]ZnMe, [Tm^{But}]ZnEH (E = S, Se) and [Tm^{But}]ZnEPh (E = O, S, Se, Te). *Chem. Commun.* **2004**, 2870–2871. [CrossRef]
35. Barth, B.E.K.; Leusmann, E.; Harms, K.; Dehnen, S. Towards the installation of transition metal ions on donor ligand decorated tin sulfide clusters. *Chem. Commun.* **2013**, *49*, 6590–6592. [CrossRef] [PubMed]
36. Márquez, C.; Hudgins, R.R.; Nau, W.M. Mechanism of host-guest complexation by cucurbituril. *J. Am. Chem. Soc.* **2004**, *126*, 5806–5816. [CrossRef] [PubMed]
37. Jeon, Y.J.; Kim, S.-Y.; Ko, Y.H.; Sakamoto, S.; Yamaguchi, K.; Kim, K. Novel molecular drug carrier: Encapsulation of oxaliplatin in cucurbit[7]uril and its effects on stability and reactivity of the drug. *Org. Biomol. Chem.* **2005**, *3*, 2122–2125. [CrossRef] [PubMed]
38. Lagona, J.; Mukhopadhyay, P.; Chakrabarti, S.; Isaacs, L. The cucurbitnuril family. *Angew. Chem. Int. Ed.* **2005**, *44*, 4844–4870. [CrossRef] [PubMed]

39. Bakbak, S.; Bhatia, V.K.; Incarvito, C.D.; Rheingold, A.L.; Rabinovich, D. Synthesis and characterization of two new bulky tris(mercaptoimidazolyl)borate ligands and their zinc and cadmium complexes. *Polyhedron* **2001**, *20*, 3343–3348. [CrossRef]
40. White, J.L.; Tanski, J.M.; Rabinovich, D. Bulky tris(mercaptoimidazolyl)borates: Synthesis and molecular structures of the Group 12 metal complexes [Tm^{tBu}]MBr (M = Zn, Cd, Hg). *J. Chem. Soc. Dalton Trans.* **2002**, 2987–2991. [CrossRef]
41. Coates, W.J.; Mckillop, A. One-Pot Preparation of 6-Substituted 3(2*H*)-Pyridazinones from Ketones. *Synthesis* **1993**, *1993*, 334–342. [CrossRef]
42. Wu, D.H.; Chen, A.D.; Johnson, C.S. An Improved Diffusion-Ordered Spectroscopy Experiment Incorporating Bipolar-Gradient Pulses. *J. Magn. Reson.* **1995**, *115*, 260–264. [CrossRef]
43. Jerschow, A.; Müller, N. 3D Diffusion-Ordered TOCSY for Slowly Diffusing Molecules. *J. Magn. Reson.* **1996**, *123*, 222–225. [CrossRef]
44. Jerschow, A.; Müller, N. Suppression of Convection Artifacts in Stimulated-Echo Diffusion Experiments. Double-Stimulated-Echo Experiments. *J. Magn. Reson.* **1997**, *125*, 372–375. [CrossRef]
45. Sheldrick, G.M. A short history of *SHELX*. *Acta Crystallogr. A* **2008**, *64*, 112–122. [CrossRef] [PubMed]